

3D-Printing Optical Components for Microscopy using a Desktop 3D-Printer

Jay L. Christopher^{a*}, Peter W. Tinning, Deepak Uttamchandani and Ralf Bauer

^aCentre for Microsystems and Photonics, Technology and Innovation Centre, University of Strathclyde, Glasgow, Scotland

*jay.christopher@strath.ac.uk

ABSTRACT

In this work, we present the results of using a commercially available SLA printer for the fabrication of a range of designs of optical components. The optical properties are compared to off-the-shelf optics, including a detailed analysis of optical transmission, part uniformity and surface quality. A post-processing refinement step is introduced whose results are benchmarked against off-the-shelf polished glass lenses to exemplify sub-hundred nanometre surface uniformity with minimal surface defects, and transmission properties as high as 85% at 638 nm for a 1 mm thick optical block without anti-reflection coatings.

Keywords: 3D Printing, 3D printed optics

INTRODUCTION

Novel imaging techniques and instruments contribute immensely to the understanding of biomedical processes and biological interactions, though often at a high equipment cost. Rapid-prototyping additive manufacturing of optical systems and components has the potential to reduce this price and availability gap. Using commercially available consumer-grade stereolithography (SLA) 3D printing technology, the creation of individual optical elements such as plano-convex lenses, solar-concentrator arrays and mirrors^[1,2] has been successfully demonstrated at a fraction of the off-the-shelf cost, whilst providing comparable optical quality and significant free-form customization potential.

While there are a variety of differing SLA printing approaches, each of them generates the structure layer-by-layer through curing of a liquid resin^[3], with the height of each printed layer defined by the type of SLA technology used. In general, printing techniques capable of achieving sub-micrometre layer and in-plane resolution, such as the 2-photon technique used by Nanoscribe^[4], or the inkjet droplet method used by Luxexcel-Printoptical technology^[5], are significantly more expensive than commercially available desktop printers which are limited to layer and in-plane resolutions in the tens to hundreds of micrometre range. This leads to the requirement of a post-processing step to create optical quality parts with these printers as the layers generate a ‘staircase effect’ which produce printed surfaces with stepping between each layer in the micron-scale^[6]. A variety of cost-effective methods to reduce the staircase effect have been demonstrated previously. These include sanding and polishing the optical element with finer and finer abrasive paper^[7] or additively filling the layer steps. The latter is done through coating processes to achieve an inverse structure for re-moulding, or to produce the optical part directly if transparent resins and coating materials are used as fillers^[1,2]. Although polishing the printed parts is the simplest technique, it is laborious and cannot easily be employed for more complex geometries or free-form surface areas, thereby negating the advantages of cost-efficient 3D-printing over traditional manufacturing of optical components such as glass lenses. The filling of the layer gaps on the other hand, either through dip-coating the surface or by spin-coating, allows compatibility with automation and flexible surface design. Both dip-coating and spin-coating fill the step profile through surface tension of a liquid resin, which can be the same as the resin used for the main part. By controlling the removal speed for dip-coating and the spin-speed for spin-coating, a controlled layer thickness can be achieved which will allow smoothing of the non-uniform surface. A further curing step of the deposited extra resin layer will then lead to an optical quality surface.

In this work we present an approach to create 3D printed optical components using a low-cost desktop 3D-printer (Elegoo Mars 2) and a spin-coating post-process step to reduce layering. We will detail the fabrication steps to reach nanometre

surface roughness and show the characterisation of printed cuboids and lenses to evaluate surface uniformity, surface roughness and optical transmission.

3D PRINT AND POSTPROCESSING METHODOLOGY

To evaluate the performance of 3D printed elements, several simple geometries were fabricated and characterised. These consisted of cuboids and plano-convex lenses. All elements were designed using Autodesk Inventor. Cuboids were designed with 12.7 by 12.7 mm faces and thicknesses of 1-5 mm to characterise the optical flatness and transmission characteristics of the resin (Formlabs Clear resin) and post-processing methodology. The cuboids were printed using an Elegoo Mars 2 printer with 10 μm layer resolution and their 12.7 by 12.7 mm surface placed flat onto a polished (to 0.3 μm) magnetic base attached to the original printer build platform. Once printed, the cuboids were removed from the magnetic base and washed in an Elegoo Mercury Plus Washing and Curing machine using IPA. The blocks were blow-dried with compressed air before the following spin-coating post-process steps. Formlabs clear resin was spun on a cleaned microscope slide at 1400RPM for 30 seconds and placed in a small low-pressure chamber at -0.95 bar for 15 minutes to ensure removal of any micro-bubbles in the resin layer. The cleaned 12.7 mm cuboid surfaces were gently placed onto the coated slide and gradually placed under vacuum again for a 30-minute period. Once all trapped air bubbles have been removed from the surface, the cuboid and slide were UV cured for 6 minutes (Elegoo Mercury Puls wash & cure). After this a scalpel was used to cut around the edges of the cuboid to cleanly remove the parts from the slides either through manual leverage or differential expansion by freezing the slide.

Printed lenses were manufactured through a similar process, and the lens dimensions were chosen to match the dimensions of a Thorlabs $\frac{1}{2}$ " diameter uncoated 20 mm focal length N-BK7 plano-convex lens. The 3D-printed lenses were printed at an angle of 70 degrees relative to the print bed to ensure best form reproduction whilst balancing issues involving layering thickness and support placement. After washing the lenses similarly to the cuboids, the supports around the edges were trimmed and the flat face of the plano-convex lens was coated first identically to the cuboids. For the curved surface, the lens was placed into a $\frac{1}{2}$ " holder in a spin coater. 500 mg of resin was deposited onto the centre of the curved surface and was spun at 1400 RPM for 10 seconds to ensure even coverage over the lens surface to fill in the steps originating from the layer-by-layer print process. The lens was then cured under UV light for approximately 3 hours.

EXPERIMENTAL RESULTS

Surface profiles

Surface profiles were obtained for each element using a Veeco NT1100 white light interferometer (for 2D surface roughness measurements) as well as a KLA Tencor Alpha-Step IQ stylus profiler (for 1D surface topology measurements). The 3D-printed cuboids were compared to a Thorlabs N-BK7 high-precision window (WG10530), with an example of the resulting 2D surface profiles shown in Figure 1.

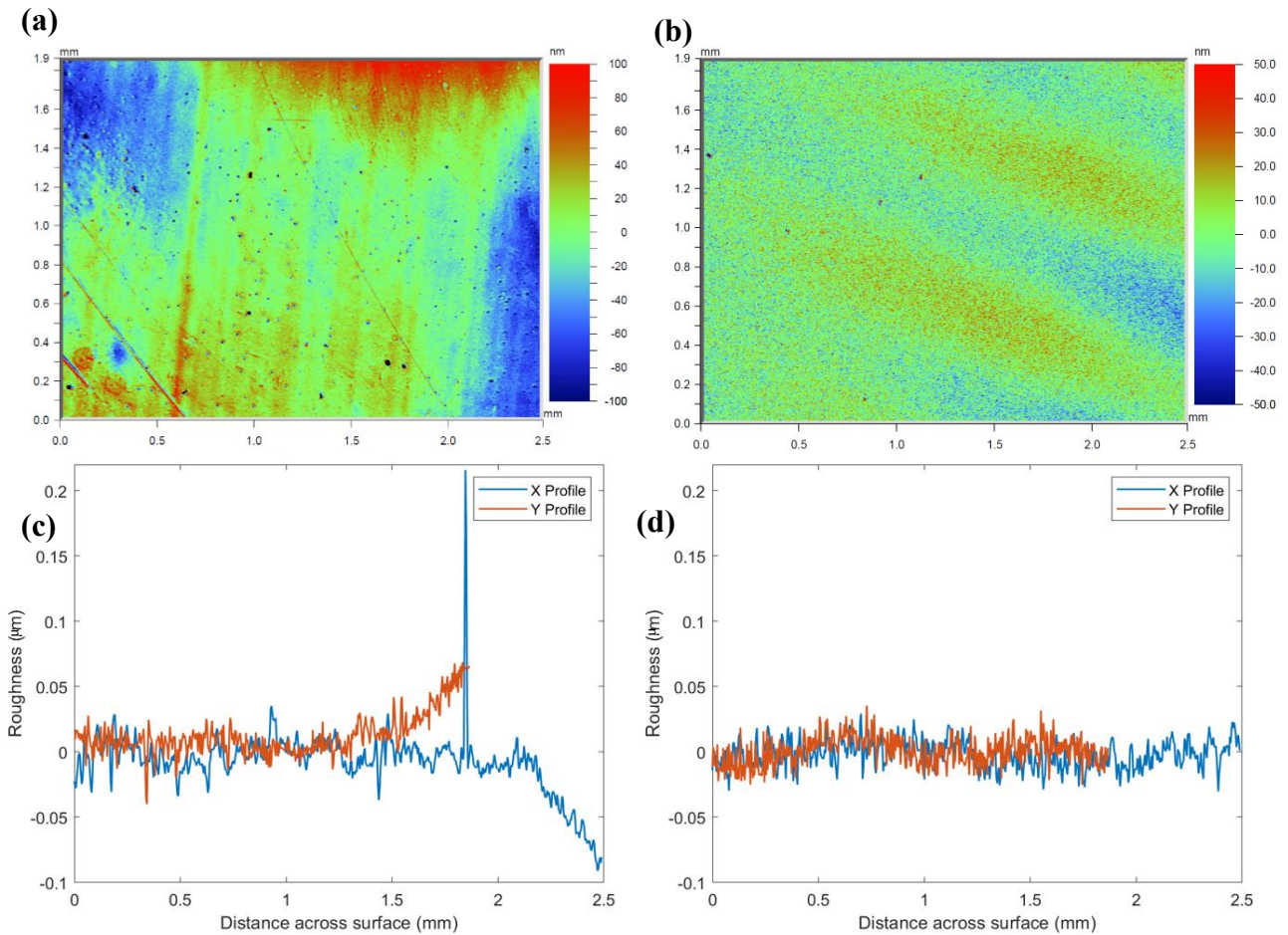


Figure 1 – (a,b) Surface roughness colourmaps obtained using the Veeco NT1100 white light interferometer of a 3D printed, post-processed flat surface and a commercially available transparent flat surface respectively. (c,d) Surface roughness plots taken from line graphs in X and Y across the centre of each colourmap respectively.

Figure 1(a) exemplifies that the average surface roughness for the 3D-print is approximately 25 nm over the imaged area, and whilst not perfectly uniform, the roughness reaches maximum values approaching 100 nm which is promising for optical flatness when imaging. Though the surface measurements were performed in a cleanroom environment and the surfaces were cleaned with IPA and blow-drying, dust particles can still adhere to the surface both before post-processing and after the curing step which can contribute outlier high value data points. To address this, the colourmap in 1(a) has been scaled to eliminate the impact of the outliers caused by objects such as dust which would increase the roughness scale causing the image to saturate into one colour around its 25 nm average. The average roughness from 1(a) is comparable to the commercially available flat BK7 window, shown in Figure 1(b) with an approximate 9 nm roughness. This sub-hundred nanometre quality is crucial to ensure clear optical transmission and minimal light scattering. The line profile in Figure 1(c) quantitatively shows that much of the reason for a slightly higher surface roughness of the 3D-print can be due to very minor regions of the surface with small particles or dust present on the surface during the surface profile scan. The cross section of the commercial optical flat window in Figure 1(d) shows the expected homogeneous surface roughness over the full measurement range. Both the commercial window and the 3D-printed cuboid show surface radius of curvatures larger than 40 m, rendering both almost perfectly flat and exceeding flatness requirements for most biomedical imaging applications.

Transmission measurements

To evaluate the transmission properties of the 3D-print resin and printed parts, measurements of the transmitted optical power were taken at multiple wavelength and thicknesses of the 3D-prints. It is recognised that scattering, material absorption and Fresnel reflections contribute to the transmissions less than 100% and the individual contributions are under analysis. Cuboids with the above shown surface profiles were used for this, which did not include anti-reflection coatings. Three different laser wavelengths covering the visible spectrum were used for this evaluation, with incident optical powers of 25 mW. The resulting optical transmission values for the varying wavelengths and thickness are shown in Figure 2, with each thickness and wavelength combination measured five times.

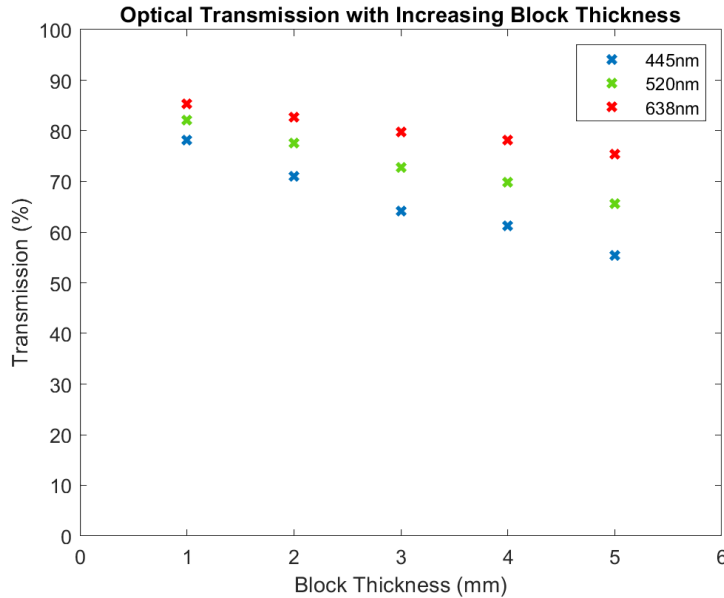


Figure 2 – Transmission characteristics of five thicknesses of optically clear 3D printed cuboids (blocks) measured at three discrete wavelengths of light

As seen in Figure 2, the transmission through each block decreases as the thickness increases, which we would expect to follow an exponential decay function similarly to the transmission through glass of increasing thickness. For blocks of 1 mm thickness a net transmission ranging from 85% at 445 nm to 78% at 638 nm can be seen, while at 5 mm the transmission drops to between 75% and 55% for the two wavelengths. The uncertainty in these percentages was found to be at most $\pm 1.2\%$.

Curvature Profiles

The surface quality and profile of the 3D-printed lenses was compared to a polished glass plano-convex lens with identical dimensions (Thorlabs LA1074). The resulting 2D roughness comparison and surface line profile comparison over a 2 mm length are shown in Figure 3, including a fit to an ideal circular surface shape.

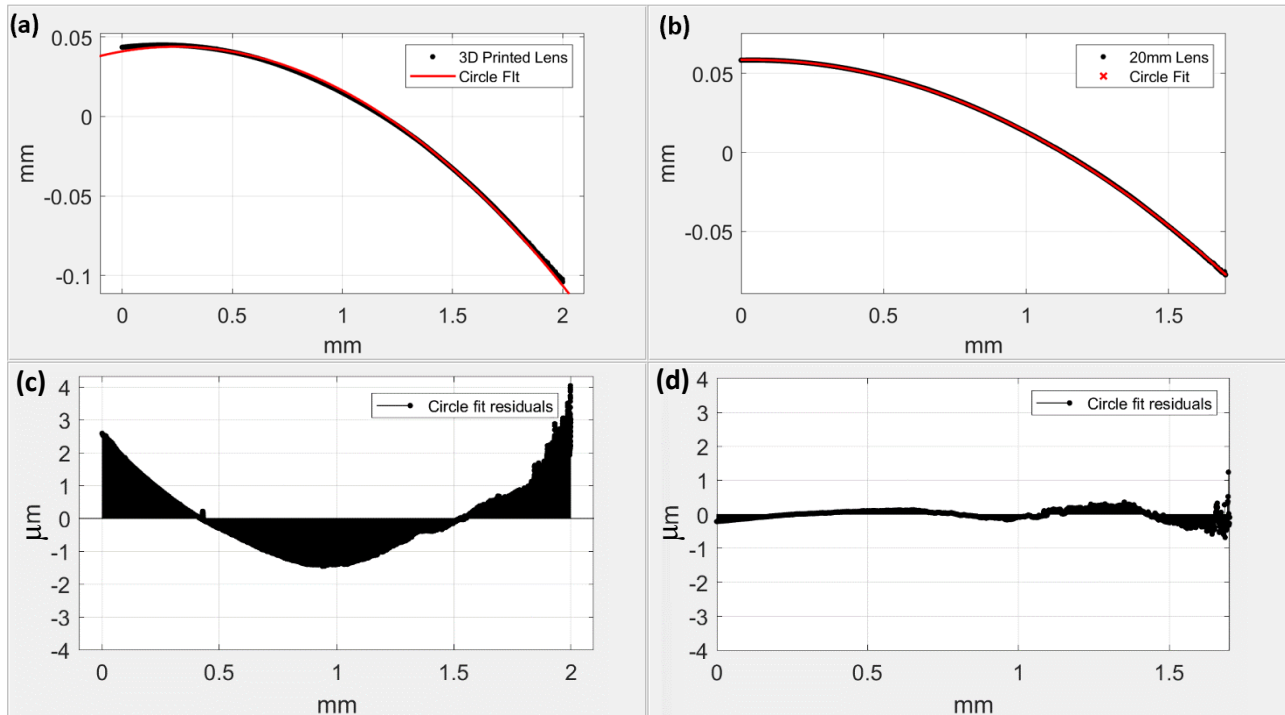


Figure 3 – (a,b) Printed and commercial lens form, obtained using the KLA Tencor Alpha-Step IQ stylus profiler, respectively with circle function to exemplify curvature. (c,d) Residuals to show surface roughness taken through the centre of each lens respectively

Both the 3D-printed lens and commercial lens profile match well with the ideal spherical surface. While nominally having the same design, the 3D-printed lens shows a slightly higher curvature and against the circular fit, with an R^2 value of 0.9994, indicating a potential small mismatch in layer height during the printing. Since the curvature nearly perfectly matches an R^2 value of 1, which is the case for the commercial lens, the curvature mismatch should not have a detrimental effect on a final image within the targeted biomedical imaging applications. The surface roughness of both parts is again comparable, with the 3D-print and commercial lens showing a residual error from the ideal parabola of 4 μm or less. In both cases the surface again conforms to the optical requirements for most microscopy applications.

Imaging

To detail the resulting overall performance of the printed lenses, Figure 4 shows the comparison of images of the printed lenses relative to the polished glass lens over graph paper.

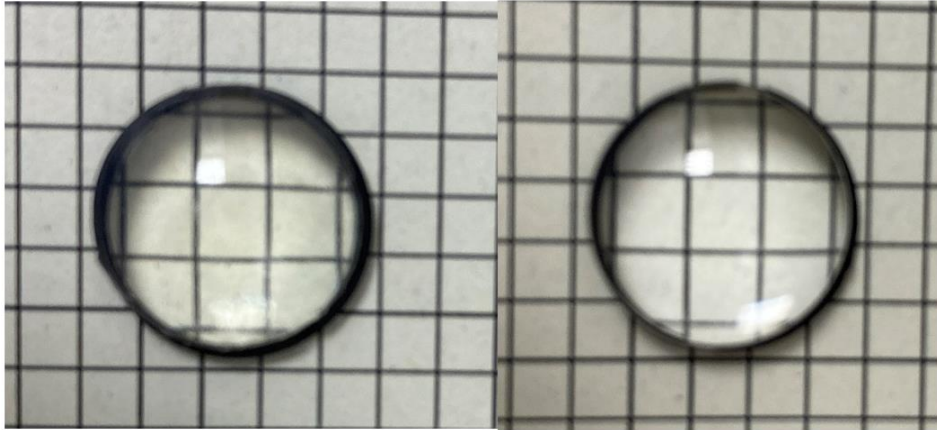


Figure 4 – Grid lens comparison with 3D printed lens (left) and commercial lens (right). For scale, the diameter of each lens is 12.7mm.

To show the focusing properties of the printed lenses, a uniform grid pattern was used as a background for white light illumination through the commercial lens and 3D-printed lens. Both lenses are placed on a 1.7 mm tall spacer to increase the magnification of the grid pattern image through the lens. Both lenses show an identical magnification and line profile, with slight bending of the lines due to imaging through a plano-convex lens. Clarity of the lines is comparable, with the 3D-printed lens showing a slightly stronger deformation and a slight yellowing due to the UV curing process of the 3D-print resin.

CONCLUSION

We have shown the production and characterisation of 3D-printed optical elements using a low-cost commercial desktop 3D-printer. The process to improve the surface profiles to an optical quality standard using a post-process step has been demonstrated and the resulting elements characterised for their surface roughness, surface profile and transmission characteristics. At all points a comparison to precision polished optical glass surfaces was given. With the confirmed print-process being optimised, the presented technique will allow creation of more complex optical shapes beyond standard polished surfaces, allowing the implementation of printed microlenses, free-form surfaces and more complex elements.

ACKNOWLEDGEMENT

We acknowledge funding from the UK Engineering and Physical Sciences Research Council (grant EP/S032606/1 and doctoral training partnership EP/T517938/1) and UK Royal Academy of Engineering (Engineering for Development Fellowship scheme RF1516/15/8).

REFERENCES

- [1] N. Vaidya and O. Solgaard, "3D printed optics with nanometer scale surface roughness," *Microsystems*

- Nanoeng.*, Vol. 4, no. 1, (2018). DOI: 10.1038/s41378-018-0015-4.
- [2] G. D. Berglund and T. S. Tkaczyk, "Fabrication of optical components using a consumer-grade lithographic printer," *Opt. Express*, Vol. 27, no. 21, p. 30405-30420, (2019). DOI: 10.1364/oe.27.030405.
- [3] S. Zakeri, M. Vippola, and E. Levänen, "A comprehensive review of the photopolymerization of ceramic resins used in stereolithography," *Addit. Manuf.*, vol. 35, page 1-3, 101177 (2020). DOI: 10.1016/j.addma.2020.101177.
- [4] S. Wu, J. Serbin, and M. Gu, "Two-Photon Polymerisation for Three-Dimensional Micro-Fabrication," *J. Photochem. Photobiol.*, 181(1), 1-11 (2006). DOI: 10.1016/j.jphotochem.2006.03.004.
- [5] B. Assefa, M. Pekkarinen, H. Partanen, J. Iskop, J. Urunen, and J. Aarinen, "Imaging-quality 3D-printed centimeter-scale lens," *Opt. Express*, vol. 27, no. 9, 12630–12637 (2019). DOI: 10.1364/OE.27.012630.
- [6] D. Rodriguez, J. Fernandez, J. Quiroga, and D. Vazquez, "Smoothing of 3D Printed Lenses," U.S. Patent 10,086,575 issued Oct. 2, 2018
- [7] A. Dudley, "Creating Camera Lenses with Stereolithography", <https://formlabs.com/blog/creating-camera-lenses-with-stereolithography/>
[Accessed: 24-Dec-2021]